MRU Cardington Technical Note No. 11

Principles, accuracy and performance of a doppler acoustic sodar

by

W.P. Hopwood

7 October 1992

Met. Office Research Unit
RAF Cardington
Shortstown
Beds, MK42 0TH

MRU CARDINGTON

Note

This paper has not been published and PMetO(Cardington) should be consulted before quoting from it.

MORU Cardington Technical Note No. 11

Principles, accuracy and performance of a doppler acoustic sodar

by

W.P.Hopwood

7 October 1992

Met. Office Research Unit
RAF Cardington
Shortstown
Beds, MK42 0TH

Note

This paper has not been published and PMetO(Cardington) should be consulted before quoting from it.

Principles, Accuracy and Performance of a Doppler Acoustic Sodar

W.P.Hopwood

Met. Office Research Unit.
Cardington,
Bedford.
MK42 0TH

August 1991

Abstract

The Doppler Acoustic Sounder is potentially a useful method of probing the boundary layer structure over long periods of time. This paper discusses the principle of operation of the device and identifies the limiting factors to its accuracy. Also presented is attempt to quantify its performance over a variety of atmospheric conditions, which indicates that the instrument's accuracy is variable upon the surface windspeed and the state of precipitation.

1 Introduction

The current physical understanding of the atmospheric boundary layer relies to great extent upon the direct measurement of the boundary layer parameters. By 'direct', it is understood that instruments measuring windspeed, temperature, etc. are placed at various heights on say a tower such as the one at Cabauw in Holland. The output from these devices is directly proportional to the quantity that they are measuring. Unfortunately, this sort of technique is very restrictive, in the sense that it is only a single point measurement and the maintenance of anumber of such instruments, together with their calibration,is insensitive. However, many boundary layers parameters may be inferred from small inhomogeneities that exist within this layer, with the assumption that they are small enough to be carried along with the mean flow. These inhomogeneities arise because of the turbulent mixing that exists within the boundary layer. their usefulness is due to their very difference from the surrounding media, in that they act as scattering centres fro wave motion propagating through the layer. Hence, by emitting a pulse of 'radiation' of the correct frequency and detecting the scattered return pulse, the velocity of the inhomogeneities can be deduced from the doppler frequency shift associated with the motion of the scatterer in the mean flow with respect to the source. This arrangement would allow a single instrument on the ground to probe the boundary layer at a number of heights simultaneously. One such instrument is a doppler acoustic sounder or Sodar. A Sodar operates by emiting pulses of sound and then 'listening' to the returns produced by the scattering of sound from turbulent fluctuations in the acoustic refractive index. These variations in the refractive index are primarly associated with turbulent fluctuations in temperature, velocity and humidity, and the intensity of the returned signal provides a measure of the intensity of these fluctuations with scales on the order of the wavelength of the sound used. Now, for a monostatic arrangement, ie. one where the transmitter and receiver are co-located, only fluctuations in temperature, and to a lesser extent humidity, are responsible for the returned signal. Observations of acoustic returns show clearly that the intensity of small scale turbulent fluctuations is not spatially uniform and many flow patterns can be seen in the lower atmosphere.

The frequency shift of the received signal relative to that of the transmitted pulse gives information on the motion of the inhomogeneities responsible for the scattering of the acoustic pulses. In most cases, the scales of these inhomogeneities are small enough for it to be assumed that they move with the same velocity as the mean wind, so the

doppler shift can be used to measure the mean wind profiles. The relation that connects the frequency change Δf_d and the wind component u in the radial beam direction is given by,

$$\Delta f_d = \frac{2u}{\lambda} \tag{1}$$

2 Principles

Acoustic waves are pressure waves as opposed to electromagnetic waves and it is worth looking at their properties.

The propagation velocity of longitudinal pressure waves through a fluid is determined by the fluid pressure, P, and the density, ρ. In the atmosphere, changes in pressure and density due to the passage of a sound wave are adiabatic, so that,

$$P\alpha^{\gamma} = constant \tag{2}$$

where α is the specific volume and $\gamma = c_p/c_v$, the ratio of the specific heats. Then, the velocity of sound, c, is given by,

$$c = \sqrt{\frac{\gamma P}{\rho}} = \sqrt{\frac{\gamma RT}{M}} \tag{3}$$

with R as the universal molar gas constant ($= 8314.32 JK^{-1}$) and M as the molecular weight of dry air ($= 28.9644 kgKmole^{-1}$). However, for moist air the molecular weight is given by,

$$M_w = 28.9644(1 - 0.38e/P) \tag{4}$$

where e is the water vapour pressure. Hence the velocity becomes,

$$c = 20.05(1 - 0.19e/P)\sqrt{T} \tag{5}$$

If the air is moving at a velocity $\vec{v}$, the velocity of sound $\vec{c}$ at a point on a wave front is

$$\vec{c}' = \vec{n}c + \vec{v} \tag{6}$$

with $\vec{n}$ as a unit normal vector to the wave front.

With the propagation velocity defined, the attenuation of an acoustic pulse must also be considered, as it is markedly different than that associated with electromagnetic pulses.

Firstly, the intensity of a acoustic/sound wave is defined as the time rate of energy passage through a unit area perpendicular to the direction of wave propagation. The attenuation of acoustic waves as they propagate through the atmosphere varies with

the frequency of the waves but it does so in a smooth, continuous manner. When small frequency ranges are considered, the intensity of a plane wave train, I, at some distance, l, from a reference plane where the intensity is I_0 is given by,

$$I = I_0 e^{-kl} \tag{7}$$

The constant k is known as the attenuation coefficient with units of inverse length. It measures the distance the wave has to travel through the medium so that its intensity falls to $1/e$ of its incident value. this coefficient is made up of three independent components, namely,

$$k = k_c + k_m + k_s \tag{8}$$

which take into account of the three types of acoustic interaction, c for classical attenuation, m for molecular absorption and s for scattering.

The classical attenuation is caused by the finite viscosity of the air, which leads to heating of the air as the sound wave passes, by radiation and conduction from the high pressure regions of the sound wave. Classical absorption, first studied by Stokes (1849) and then by Rayleigh (1896), varies with frequency as,

$$k_c = 4.24 f^2 \times 10^{-11} \tag{9}$$

from Beranek (1954). Compared with the other sources of attenuation it is very small and can be said to be negligible within audible frequencies and normal temperature and pressure. The first investigation into the cause of molecular absorption beyond that predicted classically was performed by Knudsen (1931), in seeing a marked dependence on the humidity of the air. He showed that abnormally high absorption is determined by an interaction between Oxygen and water molecules. The mechanism was later explained by Kneser (1933) as the transfer of collision-excited vibrational energy, produced by the acoustic field, from Oxygen molecules to the water vapour molecules. The energy of the excited water vapour molecules is radiated away in the infra-red. This transfer is facilitated by the near exact overlap of energy levels within the two types of molecule,but while radiative decay is not possible for the Oxygen molecules, this method of energy removal is highly favoured by water vapour. See Henderson and Herzfeld (1965) and Figure 1. Molecular absorption increases with temperature, which helps explain why, in cold climates, cases of unusually long-range sound propagation has been reported. Although refractive ducting between sharp temperature inversions formed in cold conditions may also be important. For example,

For a frequency of 2KHz in air at 20C with 15classical absorption coefficient is $k_c = 1.7 \times 10^{-4} m^{-1}$. From Figure 1 $k_m = 6 \times 10^{-3} m^{-1}$. That is 35 times bigger.

Acoustic echo sounding is possible because sound is scattered from a probing acoustic beam by temperature and wind turbulence. Obviously, if energy is scattered from the beam, the intensity of the beam will decrease.

The theory of scattering of sound caused by velocity fluctuations in the atmosphere has been by Lighthill and Kraichnam (1953), while Bachelor (1957) has treated the scattering caused by temperature inhomogeneities. Monin (1961) showed that the fraction, $\sigma(\theta)$, of the incident power scattered from a unit volume per unit incident into a solid angle is,

$$\sigma(\theta) = \frac{32\pi \cos^2\theta}{\lambda^4}\left[\frac{\Phi(v)(\frac{4\pi}{\lambda}\sin\theta/2)}{c^2} + \frac{\Phi(T)(\frac{4\pi}{\lambda}\sin\theta/2)}{4T^2}\right] \tag{10}$$

where the first term in the bracket is due to velocity and the second is due to temperature, θ is the scattering angle measured from the direction of propagation of the incident wave; λ is the wavelength of sound for average temperature T; $\Phi(v)$ is the the dimensional spectral density of fluctuations in wind velocity; $\Phi(T)$ is the three dimensional spectral density for fluctuations in temperature and T is the average temperature within the scattering volume. Both $\Phi(v)$ and $\Phi(T)$ are evaluated at the spatial scale λ' where,

$$\lambda' = \frac{\lambda}{2\sin\theta/2} \tag{11}$$

Little (1970) referred to the term $\frac{4\pi}{\lambda}\sin\theta/2$ as the effective wavenumber at which the acoustic radar scattering through θ interrogates the medium. In deriving (10) it has been assumed that the wind and temperature fluctuations are uncorrelated and homogeneous, that the atmosphere is locally isotropic and that humidity fluctuations are not important. Scattering from humidity fluctuations would typically be 2-3 orders of magnitudes less than the scattering by temperature and wind fluctuations, therefore it may be ignored. The other assumptions are not so clearly acceptable, but experience has shown that it does provide a first order approximation to sound scattering in the boundary layer.

Kolmogorov (1941) studied the local structure of turbulence in an incompressible viscous fluid at very large Reynolds number. He concluded that in such a fluid, energy

is partitioned among the turbulent eddies in proportion to $k^{-5/3}$, where k is the wave number. Using the Kolmogorov spectrum of turbulence, equation 59 above may be written as,

$$\sigma(\theta) = 0.055\lambda^{-1/3}\cos^2\theta[\frac{C_v^2}{c^2}\cos^2\theta/2 + 0.13\frac{C_T^2}{T^2}](\sin\theta/2)^{-11/3} \tag{12}$$

where C_v and C_T are the velocity and thermal structure parameters which are defined by,

$$C_v^2 = \overline{[\frac{v(x) - v(x+\Delta x)}{(\Delta x)^{1/3}}]^2} \tag{13}$$

$$C_T^2 = \overline{[\frac{T(x) - T(x+\Delta x)}{(\Delta x)^{-1/3}}]^2} \tag{14}$$

with v(x) and T(x) as the instantaneous windspeed and temperature at position x and, $v(x+\Delta x)$ and $T(x+\Delta x)$ are those at $(x+\Delta x)$. It is apparent from the equation for $\sigma(\theta)$ that scattering is weakly dependent upon the wavelength (λ), and that short waves are scattered more strongly than long waves. Also, scattering from wind fluctuations is a function of,

$$\cos^2\theta\cos^2\theta/2[\sin\theta/2]^{-11/3}$$

which vanishes at $\theta = \pi/2$ and $\theta = \pi$. Hence, neither backscattering nor scattering normal to the direction of sound propagation should be expected from mechanical turbulence. Scattering from temperature inhomogeneities may be expected at $\theta = \pi$ but not at $\theta = \pi/2$. Thus, the equation for $\sigma(\theta)$ for backscattering ($\theta = \pi$) reduces to,

$$\sigma(\pi) = 0.055\lambda^{-1/3} \times 0.13\frac{C_T^2}{T^2} = 0.00715\lambda^{-1/3}\frac{C_T^2}{T^2} \tag{15}$$

This defines the degree of scattering that might be expected under certain refractive index inhomogeneity conditions defined by the structure parameter.

3 Experimental: Derivation of Wind Vector

The derivation of a wind vector is affected by two limitations: firstly although the atmosphere provides scattering centres for the acoustic beam to interact with it also acts as a limiting factor on the beam as a whole. Secondly, the method of sampling data limits the performance of the instrument. Both are discussed below.

3.1 Atmospheric Limitations

In a similar way to Radar devices, the useful power returned from scattering centres in the atmosphere, can be said to be,

$$P_r = P_t \frac{\sigma c \tau A_e L}{2R^2} \tag{16}$$

where $\sigma = \sigma(\pi)$, τ is the sound pulse length, A_e is the effective cross-sectional area, L is a term taking into account the attenuation throughout the round trip and R is the target volume range. Considering the power levels an acoustic sounder must respond to, the theoretical limit is the acoustic noise power generated by the random thermal motion of atmospheric molecules. Under most conditions, the noise of the wind and other external factors will exceed the theoretical limits; discussed in the last section. The acoustic power return for a nominal transmitted power of twenty acoustic watts may range from near the theoretical limits at ranges of 100m to 1km for non-turbulent regions, to 60db or 70db above the noise limit for an atmosphere with a strong thermal structure function at a range of 50m. Therefore, it is necessary that an acoustic sounder system be capable of responding over an extremely wide dynamic range.

Now, substituting $\sigma(\pi)$ into the returned power equation 65 from a monostatic sodar, leads to,

$$P_r = \frac{P_t A_e}{R^2} \times 0.0072 \lambda^{-1/3} \frac{C_T^2}{T} L \frac{c\tau}{2} \tag{17}$$

The absorption, as it is cumulatory and exhibits an exponential decay behaviour, can be thought of as $e^{-2R\alpha}$ where α is the absorption coefficient defined earlier for molecular and humidity absorption and R is the range. Also, as $\lambda = 1/k$ with k as the wavenumber, this gives,

$$P_r = const \times \frac{P_t A_e}{R^2 e^{-2R\alpha}} \frac{C_T^2 k^{1/3}}{T} \frac{c\tau}{2} \tag{18}$$

It has been seen that the molecular absorption term is strongly dependent upon frequency and the relative humidity of the air. For example, for still air at 20C and 50at 1.2kHz reduces the power in the beam by a factor of 2.5 per km. At 4kHz, the reduction is by a factor of 100 per km. Consequently, for a given output power and all other things being equal, the range of the acoustic sounder should increase with a reduction in operating frequency. In order to generate a directional beam and reduce the amount of noise generated close to the surface reaching the receiver, the size of the antennae must also increase for a lower operating frequency. So there is a link between the physical size of the antenna array of an acoustic sounder and the height range it is meant to cover.

Looking at the temperature structure function, C_T^2, it measures the intensity of small scale turbulent fluctuations in temperature. Values of C_T^2 in the atmosphere vary over several orders of magnitude. Caughey and Palmer (1979) found values in the summertime convective boundary layer varying from $10^{-2}C^2m^{2/3}$ near the surface $10^{-4}C^2m^{2/3}$ above the capping inversion. For a wintertime 'convective' boundary layer with a surface heat flux of about $10Wm^{-2}$, C_T^2 is about 1.5 orders of magnitude smaller than in the summer boundary layer. Meanwhile, in the nocturnal boundary layer they may be typically, $10^{-3}C^2m^{2/3}$. Variations in C_T^2 can have a strong effect on the energy at the receiver and consequently the performance of the acoustic sounder.

Putting the following values into the radar equation 66:
$C_T^2 = 10^{-3}C^2m^{2/3}$
T=280K
$P_0 = 50W$
$k = 32m^{-1}$
Then it gives a return intensity at the antenna from a range of 500m equal to about $10^{-14}Wm^{-2}$, ignoring absorption and taking the Antenna factor to be $\sim 10^{-3}$ with an antenna area of $\sim 1.1m$. This small return signal, which is well below the threshold of hearing ($\sim 10^{-12}Wm^{-2}$) indicates that ambient noise is likely to have a significant effect upon performance.

3.2 Technical Limitations

Besides the magnitude of the received power there are other more mundane limitations that effect the Sodar's performance in deriving a wind vector. For a range gated system, the receiver is disconnected from the antenna just before the transmission of a pulse, to prevent its circuits from being overloaded, and reconnected a short time after the pulse has been transmitted. As backscattered energy from lowest levels may arrive when the receiver is disconnected, the echoes very close to the surface will not be measureable. the actual lowest height obtainable height therefore is determined by the length of the transmitted pulse and the system recovery time. Echoes are received from all heights within the range of operation of the profiler, Th received signal is spread out temporaly, with echoes from the lower heights arriving before those from the greater heights. The system can be made to to sample ehoes from equally spaced heights by measuring the returned signal after equal time intervals. This is known as *range gating*. Now, as the transmitted pulse has finite length, at any instant the received signal is coming from a volume of the atmosphere that is at a spread of ranges rather than a single point at a specific range as in Figure 2. This spread or resolutionis equal to half the pulse length. Usually the sampling interval employed in range gating is set equal to the resolution to ensure that the sample points are independent of each other. Also the transmitted energy is not only confined to a specified pulse length but concentrated into a beam. The angular width of the beam depends upon both the effective area of the antenna and the operating frequency of the profiler. As the beam needs to be narrow, either a large antenna or high operating frequency is required.

The profiler transmits energy within a narrow band of frequencies. If the scattering volume has a component of motion toward or away from the beam the return signal will be doppler shifted and hence a radial velocity can be calculated from the magnitude of the doppler shift. However the radial velocity in one direction is not enough to define the complete wind vector, three directions are needed. To solve this sodars use three beams: one pointed vertically and two tilted at right angles to each other subtending a third angle with the vertical beam. This angle is small enough for the sampling volumes to be close to each other and hence represent the same flow regime. The data that returns is restricted in several ways. The rate at which the acoustic pulses are transmitted, the Pulse Repetition Frequency or PRF, limits the range over which heights can be unambiguously determined. If the PRF is too high the echoes will overlap, that is, echoes will start to be received from one pulse while echoes from the previous pulse are

still arriving as in Figure 3. This is referred to as *Range Alaising*, as an echo from a distant scatterer masquarades as one from a much closer range gate. The time between the pulse must therefore be at least as long as the time delay between the transmission of a pulse and the reception of an echo from the geatest height expected for a useful return.

Once the scattered pulses return, for each range gate, several hundred samples are gathered and transformed into frequency space using a *Fast Fourier Transform* (FFT) similar to that shown in Figure 4. Four quantities are measured from the spectrum: the background noise power and average noise level, the signal power, the average doppler shift of the peak and the width of the peak. The power return P_r and the width of the peak W_f at each range gate are measures of the degree of turbulence, such that, the power return depends upon the population of scatterers and the peak width indicates the turbulent intensity. For some range gates a peak may be seen at the centre of the spectrum. This is due to reflections from solid, stationary targets that surround the instrument on the ground, known as *ground clutter*. The shift of the peak from its central position indicates the doppler shift that has occured, for example the shift associated with a target moving toward the instrument in shown in Figure 4. The noise can be caused by a number of effects more notably ambient site noise and the inherent electronic noise from within the system. It causes uncertainty in the measurements but can be compensated for by integration techniques. Two types of integration are used for each range gate, those computed in the time and in the frequency domains.

Time domain averaging consists of taking the mean of several consecutive samples in time before applying the FFT.

Frequency domain, or spectral averaging, involves calculating the mean spectrum from several consecutive spectra after the FFT has been applied.

Time domain averaging has the effect of reducing the noise and the computational load of the FFT. However, it limits the range of doppler shifts and thus radial velocities that can be detern=mined unambiguously. The effective sampling rate is the pulse repetiton frequency, PRF, divided by the number of samples in the time domain average. The number of samples used in the average depends upon the maximum winds expected. Spectral averaging makes the peak in the returned signal better defined. This leads to more reliable determinations of the power received, the doppler shift and the spectral

width. Its disadvantage is that it reduces the time resolution of the final results. if there were no noise present, it would take only a few seconds to obtain a reliable spectrum, but if noise is present then many spectra have to be averaged, giving a time resolution of minutes. The procedure is outlined in Figure 5.

3.3 Derivation of Wind Vector

Operationally, after the pulse has been transmitted, the echo is sampled at the specific times or range gates that correspond to predetermined heights. If t is the time between transmission of the pulse and the range gate sample time, the corresponding range, r, is,

$$r = \frac{ct}{2} \tag{19}$$

As was mentioned earlier for each range gate echoes are received from a spread of ranges. The spread of ranges, Δr, is the range resolution, so

$$\Delta r = \frac{c\tau}{2} \tag{20}$$

For example, $\tau = 100ms \Rightarrow \Delta r = 16.5m$. The height assigned to each resolution cell is the mid-point of that cell. It is desired that the range resolution be as small as possible, but there are other considerations when thinking about this: One is the amount of energy transmitted, for a shorter pulse will contain a smaller amount of energy and therefore the maximum height that yields usuable echoes will be low. Another consideration is the bandwidth, as short pulses will contain a wider spread of frequencies than longer pulses. The bandwidth of transmitted frequencies is approximately equal to the reciprocal of the pulse length. Thus, a $100ms$ pulse length corresponds to a bandwidth of about 10Hz.

Once the scattered signal has been received then each beam undergoes a wealth of doppler processing. In order to fully determine the doppler shift in both magnitude and sense, a stable local oscillator has to be offset from the transmitted frequency by a known amount. The doppler shift is,

$$f_d = -\frac{2V}{\lambda} \tag{21}$$

The measurement of f_d gives the radial velocity of the target. The phase detection of the back-scattered signal using the transmitted signal as a reference, known as *Bipolar*

Video, gives the I (in phase) and Q (quadrature, $\pi/2$ phase difference) components of the signal. The radial windspeed, but not the direction, is therefore contained in either the I or Q component, where,

$$I(t) = \frac{|A|}{\sqrt{2}} u(t - \frac{2r}{c}) \cos(\frac{4\pi r}{\lambda} - \psi + \psi_i) \tag{22}$$

and,

$$Q(t) = -\frac{|A|}{\sqrt{2}} u(t - \frac{2r}{c}) \sin(\frac{4\pi r}{\lambda} - \psi + \psi_i) \tag{23}$$

where,
2r is the total path traversed by the incident and scattered waves.
A is the voltage amplitude.
c is the speed of sound.
ψ_i is the phase shift produced by the scattering target.
ψ is the phase of the transmitted wave.
$\frac{4\pi r}{\lambda} + \psi_i$ is the phase of the received signal.

The sum of I^2 and Q^2 equals the input power averaged over the signal cycle, and the I and Q pairs are a time series sample of the doppler shifted signal. Fourier analysis of this series gives the power density (doppler) spectrum using FFT's and the velocity spectrum $S(V)$ using the notation of Burgess and Ray (1986). The integral of the spectrum is the reflectivity and the zeroth moment of the spectrum. The mean velocity $\bar{V}$ is the first moment of the spectrum, such that,

$$\bar{V} = \frac{\int V S(V) dV}{\int S(V) dV} \tag{24}$$

Once the radial velocities have been deduced at each specific height, then the calculation of the wind vector can begin. For each height, the radial velocities from the three beams are combined to calculate the zonal, meridional and vertical components u,v and w. If the beam orientated to the east at zenith angle θ_1 (beam 1), to the north at zenith angle θ_2 (beam 2) and to the vertical (beam 3); the radial velocities along these beams are.

$$v_1 = u \sin\theta_1 + w \cos\theta_1 \tag{25}$$

$$v_2 = v \sin\theta_2 + w \cos\theta_2 \tag{26}$$

$$v_3 = w \tag{27}$$

Normally, $\theta_1 = \theta_2 \sim 15°$ and from the measured v_1, v_2, v_3, u,v,w are calculated. If the orthogonal beams 1 and 2 are not oriented east and north, but rotated clockwise at an angle ϕ, then their radial velocities are,

$$v_1 = u' \sin\theta_1 + w \cos\theta_1 \tag{28}$$

$$v_2 = v' \sin\theta_2 + w \cos\theta_2 \tag{29}$$

where u' and v' are the horizontal velocities in the planes of the beams, that is, rotated ϕ to the east and north directions. Using u' and v' defined in this way the u and v components are found from,

$$u = u' \cos\phi + v' \sin\phi \tag{30}$$

$$v = u' \sin\phi + v' \cos\phi \tag{31}$$

This system, however, operates on the assumption of homogeneity in the wind field over the spatial separation of the three beams.

4 Performance of the Doppler Sodar

As has been outlined in the previous section, the performance of an acoustic sounder can be limited by a number of factors. Here, using data from a Remtech three-axis monostatic sodar situated at Cardington in Bedfordshire, these limitations to performance were investigated. The site where the sounder was situated is fairly open and the surrounding terrain between directions of 200 degrees and 330 degrees is approximately homogeneous with a roughness length of the order of centimetres. The data used in this analysis was taken for eight consecutive months between July 1988 and March 1989 at heights of 60m, 100m, 140m and 180m. Also, acting as a comparison instrument, a sonic anemometer was logging data at a height of 20m throughout this period. In addition, data taken at Cabauw in the summer of 1983 with a similar instrument, will be shown as a comparison.

The performance of this instrument can be assessed in two ways: the accuracy of its derived wind speeds and directions, and the range up to which reliable data is obtained. Both of these aspects are affected by environmental conditions close to the instrument.

4.1 Accuracy

Before discussing accuracy it is interesting to look at some data that shows that the doppler principle works. Figure 6 shows the acoustic sounder windspeed and direction at 60m compared to measurements at 20m made by sonic anemometer with time for one particular month within the period. The sounder winds are clearly larger than the sonic measured windspeeds but this can be explained by the difference in measurement heights. The plots do however show broad agreement which is encouraging.

Looking at this in more detail, Figure 7(a-c) shows the sounder 60m windspeed plotted against the 20m sonic windspeed with the rms deviations plotted on the points. For each of the three month segments shown the typical rms error in windspeed was about $1ms^{-1}$ which is significantly larger than manufacturers quoted accuracy of $0.3ms^{-1}$. For wind direction, which is shown in Figure 8(a-c), each segment shows a rms error of approximately 15-25 degrees compared to the quoted accuracy of 3 degrees.
Also, other independent comparisons have been carried out, one of these was at Card-

ington (1986) and involved compared the sounder measurements to those provided by the tethered balloon facility documented by Lapworth and Mason (1989). The results of their windspeed and direction comparisons is shown in Figures 9 and 10 with data taken from various heights. These again show a windspeed error of about $1ms^{-1}$ and direction errors of about 10-20 degrees, in agreement with the present data.
In summer 1983 a comparison between an Remtech acoustic sounder and tower measurements was also carried out at Cabauw in Holland, Beljaars (1985). The results of this experiment are shown in Figure 11. These also show an error in windspeed of about $1ms^{-1}$ and in direction, a spread of about 10-20 degrees. Now, judging by the difference between these measured errors from various studies being markedly larger than the manufacturers quoted accuracy, it suggests that there are other factors that influence the accuracy.

If stability is considered then, as shown in Figure 12 and Figure 13 for 60m and 100m, the rms deviations appear to be smaller in stable conditions than in neutral and unstable stabilities. This phenomenon also appears in the data obtained at Cabauw confirming the result.

To understand these results the method by which the sodar measures the mean wind has to be re-considered. The pulses provide discrete measurements of the radial velocity and will be taken from a random time series with some standard deviation σ, which because of the near vertical orientation of the antennae will be similar in magnitude to the standard deviation of the vertical velocity σ_w when conditions are stationary. The mean of the radial speeds obtained from the validated pulses will have a standard error of $\sigma/\sqrt{N}$, where N is the number of validated pulses. The standard error of the horizontal component derived from this mean radial speed will be $\sqrt{(2)}/\sin 18$ larger. The factor of $\sqrt{2}$ arises because the horizontal components are obtained from radial speeds measured independently by the vertical and tilted antennae. For the radial speed obtained from a pulse to be used in calculating the average windspeed the Signal to Noise Ratio of the returned signal must be greater than some threshold. Since stable conditions tend to occur at night, when the ambient noise levels are less, there may be a greater number of pulses validated than during the daytime. Further, the level of turbulence tends to be smaller in stable conditions compared to neutral/unstable conditions and, because the length scales are also smaller the effect of volume averaging reduces the effective turbulence level even more. These effects will reduce the standard error of the mean in stable conditions compared to unstable conditions. The implication

of this is that the accuracy of the sodar may be limited by statistical sampling errors and will, therefore, depend to some extent upon the prevailing conditions. Also it means that the manufacturers quoted accuracies should be looked upon with some caution.

4.2 Range

After accuracy the next important performance indicator is the maximum height from which valid winds are returned. Figure 14 shows the percentage of profiles which return winds from heights at or above a given height h. The total number of profiles used to construct this curve was 1200. It can be seen that about 95% of winds from 300m and above, but only 40% from 500m or above do so.The difference can be seen between the returns obtained at night and those from daytime. The full curve is reproduced from the manufacturers specification given for an ambient noise of 45dBA. This is equivalent to a level of noise corresponding to a quiet street or quiet conversation. From this it might be expected that there might be a greater recovery from higher levels than is observed. However, the small size of the backscattered signal implies that ambient noise is going to be an important factor in determining the sodar range. Cardington is generally fairly quiet, but the noise levels are not quantatively known.

One common source of noise mentioned earlier is that generated by the wind. Figure 15 shows a scatter plot of range versus 20m windspeed from the sonic anemometer. The plot suggests that the range is systematically reduced when the low level wind exceeds $10ms^{-1}$, with maximum ranges of 200m when the 20m wind is $\geq 16ms^{-1}$. This is within the manufacturers specifications. It is worth noting that it is the low level windspeed that is important here. The sodar will, for example, return winds of $20ms^{-1}$ from 500m as long as there is sufficient shear to ensure that the low level wind is not too high. However, whilst the effect of high winds is important it has a relatively minor impact on the curve shown in Figure 14 due to the small fraction of the time occupied by such speeds. Another mechanism for 'range-loss' is required.

A reduction in range may also occur if the backscattered signal is very small because small scale turbulence is absent, that is C_T^2 is small. This situation may occur, for example, in the smooth flow above a nocturnal inversion. To illustrate this, Figures 16 and 17 shows the range over two days, the 9th and 10th of August 1988. The range over the two days shows a marked diurnal variation and is very much reduced on the second

night. This appears to be due to the formation of a strong surface inversion, the height of which deduced from the echo strengths recorded on the sodar facsimile trace. As the morning of the 10th progresses the inversion height increases closely followed by the sodar range. However, it should not be concluded from this example that winds cannot be obtained above inversions since the magnitude of C_T^2 depends upon many factors and the ambient noise levels will also be important. The C_T^2 effect may be responsible for the occurence of low ranges at windspeed below $4ms^{-1}$.

It also should be noted that the range used here refers to the highest level from which validated wind is returned. This does not mean that winds are present at all lower levels or that the wind at the highest level is actually correct. Winds that are obviously incorrect have been noted when the windspeed close to the surface is high. These incorrect winds are always very low which is what might be expected in the presence of a high level of white noise.

Another example of noise is that generated by falling rain as it hits the parabolic reflector within the sodar antenna. No quantative study has been performed on this aspect suffice to say that it has been noted that in light rain the sodar performs unaffected, but if the rainfall becomes heavy then the although the winds are validated at most ranges they are very inaccurate, possibly due the sodar seeing doppler shifts from falling rain drops of the correct scale.

4.3 Example of Use

The wind near the ground is well described by Monin-Obukhov similarity theory. It is in the nature of similarity theories to be vague as to the precise range of the relevant parameters for which they are valid, in particular it would be useful to know over what height range similarity profiles can be used. Also there are questions as to the utility of the profile forms in inhomogeneous areas. It has been suggested that Monin-Obukhov profiles can be used in inhomogeneous terrain if an effective roughness length, that may vary with height, is specified. Workers such Wieringa, have suggested how much such an effective roughness might be, and whether it applies to situations where stability is important. If the similarity theory can be used in real terrain it is important to have some idea of the accuracy of the winds calculated.

Cardington, as has been mentioned earlier is a fairly simple area, flat and rather open. As well as the sodar wind profiles, turbulent statistics are available from a sonic anemometer mounted upon a 20m high mast. These allow effective roughness lengths to be determined and stability information to be assessed. Over a span of directions around 240 degrees the value is $z_0 \sim 0.7cm$. This corresponds to open fields with scattered bushes and buildings, although immediately around the instrumentation is smooth and grass covered. Figure 18 shows U(h)/U(20) against heights for neutral conditions with the appropriate logarithmic profiles marked. It is clear that the measured profiles depart from the logarithmic profiles above 60m. This departure maybe due to inhomogeneities in the upstream flow or other boundary layer effects particulary when the boundary layer depth becomes significant. When stable conditions are considered the departure from the similarity profiles is even more pronounced and is directly related to the stabilisation. So far results from this study suggest that acoustic sounders may be very well suited to study complex terrain.

5 Summary

Acoustic sounders provide an excellent method of observing the boundary layer remotely over prolonged periods of time. Maintenance of such a system is simple as the transmission and reception technology is relatively straight forward and reliable. However they suffer from limits in performance mainly attributed to their use of acoustic waves being particulary vulnerable to increases in background noise generated by increasing windspeeds. This limits their range and can make them non operational.

An undiscussed possible limitation of their use is in rain, as it will cause an increase in background noise, coupled with a deception of the doppler processing due to the fact that raindrops also act as large acoustic scattering centres which do not travel with the mean wind. This topic will be an item of future study.

References

Batchelor,G.K 1957 Wave Scattering due to Turbulence *Proc. Sym. Naval Hydro., NAS-NRC Publ.*, **515** pp409-430

Beranek,L.L. 1954 Acoustics New York, McGraw-Hill pp 481

Beljaars,A.C.M. 1985 Verification of Doppler Sodar Measurements *KNMI report*

Energy Research Unit 1989 New and Novel Measurement Techniques Applied to Wind Energy R and D *SERC*

Haugen,D.A. and Kaimal,J.C 1975 Use of an Acoustic Sounder for Optical Tracking Applications *USAF Technical Note*

Henderson,M.C. and Herzfeld,K.F. 1965 Effect of Water Vapour on the Napier Ferquency of Oxygen and Air *J. Acous. Soc. Am.*, **37** pp986-988

Holmes and Hunt 1988 Remote Sensing Atmospheric Winds *Applied Optics*

Kneser,H.O. 1933 The Interpretation of the Anomalous sound-absorption in Air and Oxygen in terms of Molecular Collisions *J. Acoust. Soc. Am.*, **5** pp122-126

Knudsen,V.O. 1931 The effect of humidity upon the absorption of sound in a room, and a determination of the coefficients of absorption of sound in Air *J. Acoust. Soc. Am.*, **3** pp126-138

Kolmogorov,A.H. 1941 The local structure of turbulence in and incompressible viscous fluid for very large Reynolds numbers *Dokl. Akad. Nauk. SSSR*, **30** p301

Kraichnan,R.H. 1953 The scattering of sound in a turbulent medium *J. Acoust. Soc. Am.*, **25** pp1096-1104

Lighthill,M.J. 1953 On the energy scattered from the interaction of turbulence with sound or shock waves *Proc. Camb. Phil. Soc.*,**49** pp531-555

Little,C.G. 1969 Acoustic methods for remote probing of the lower atmosphere *Proc. IEEE*, **57** 4 p571

Monin,A.S. 1961 Characteristics of the scattering of sound in a turbulent atmosphere *Sov. Phys. Acoust.*, **7** pp370-372

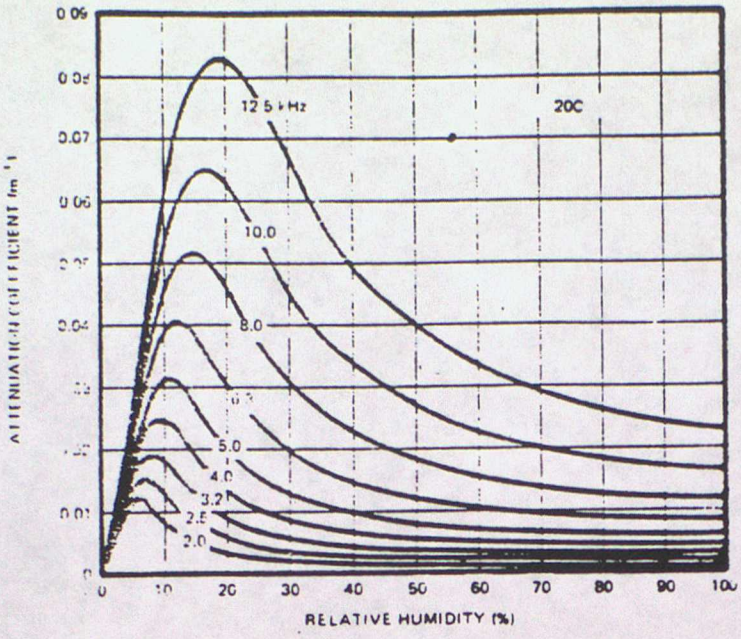

Figure 1: Absorption by water vapour

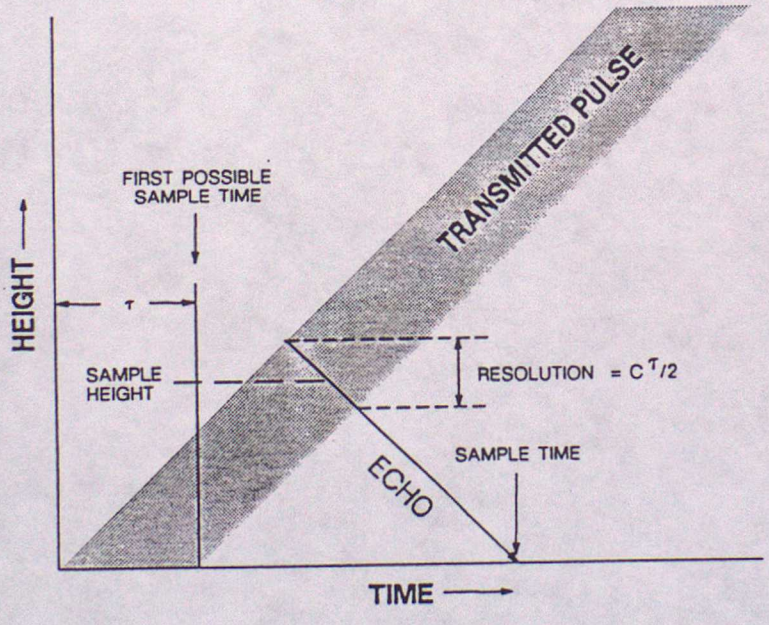

Figure 2: The echo received at any range gate corresponds to a range of heights, this is the resolution. It equals half the pulse length. The height is assigned to centre of the cell

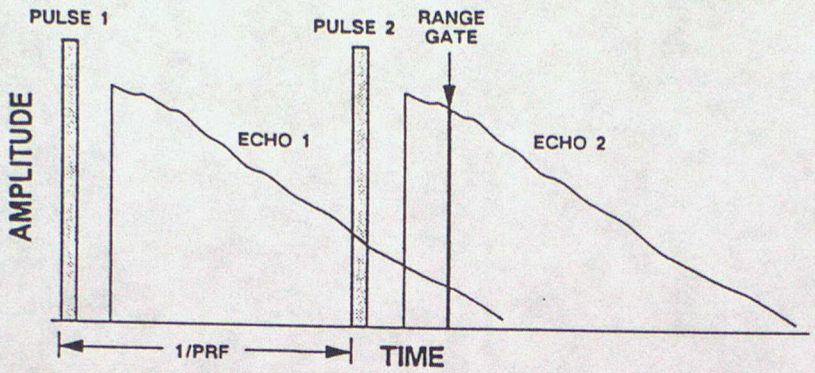

Figure 3: Example of PRF being too large. Echoes are still being received from the 1st pulse after those from the next one start to arrive. The arrowed range gate would contain data from two different heights. Range Aliasing.

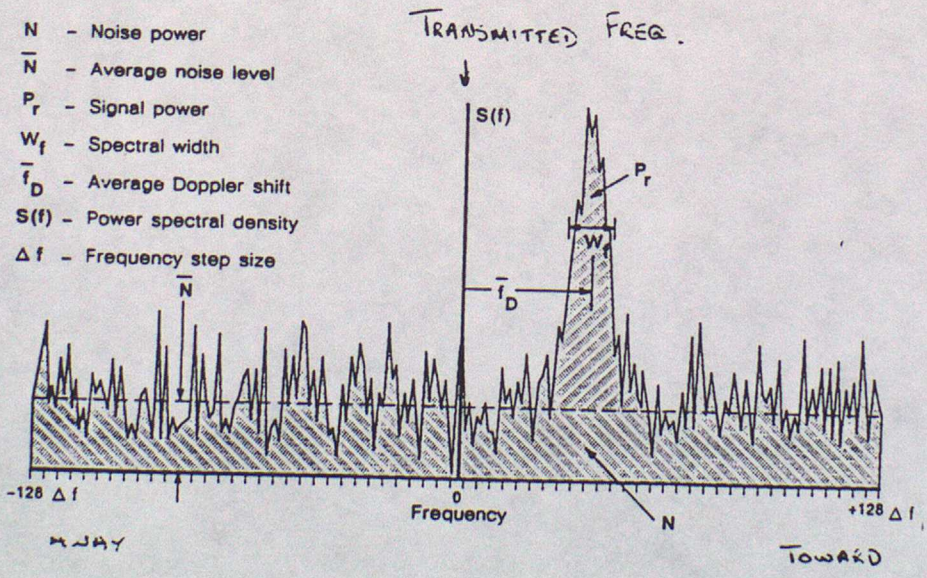

Figure 4: Power Spectrum

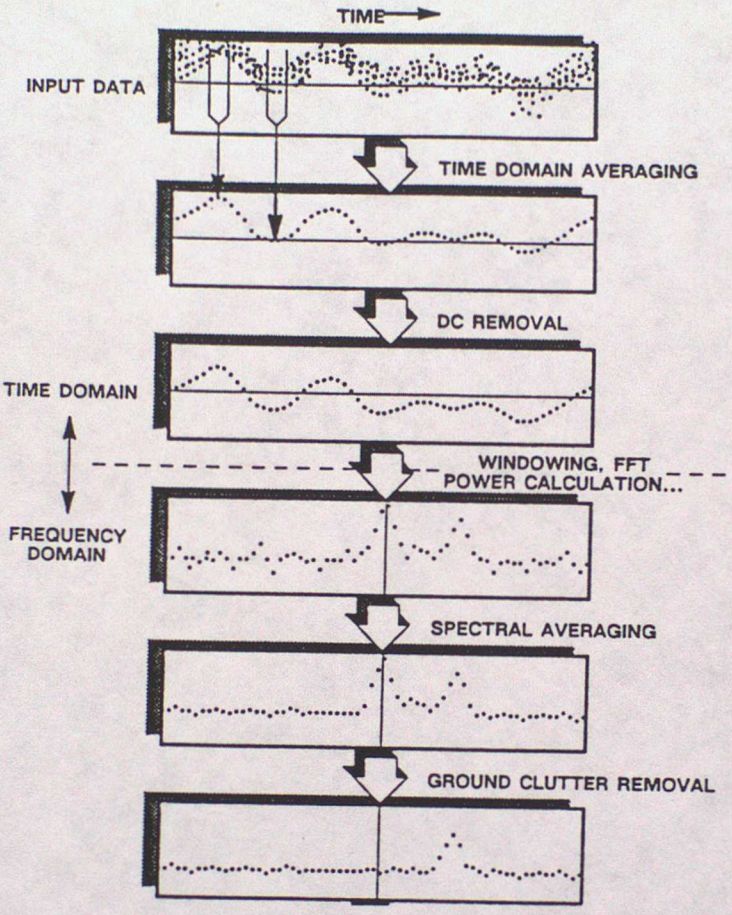

Figure 5: The processing steps used in computing wind data

Figure 6: Velocity against time

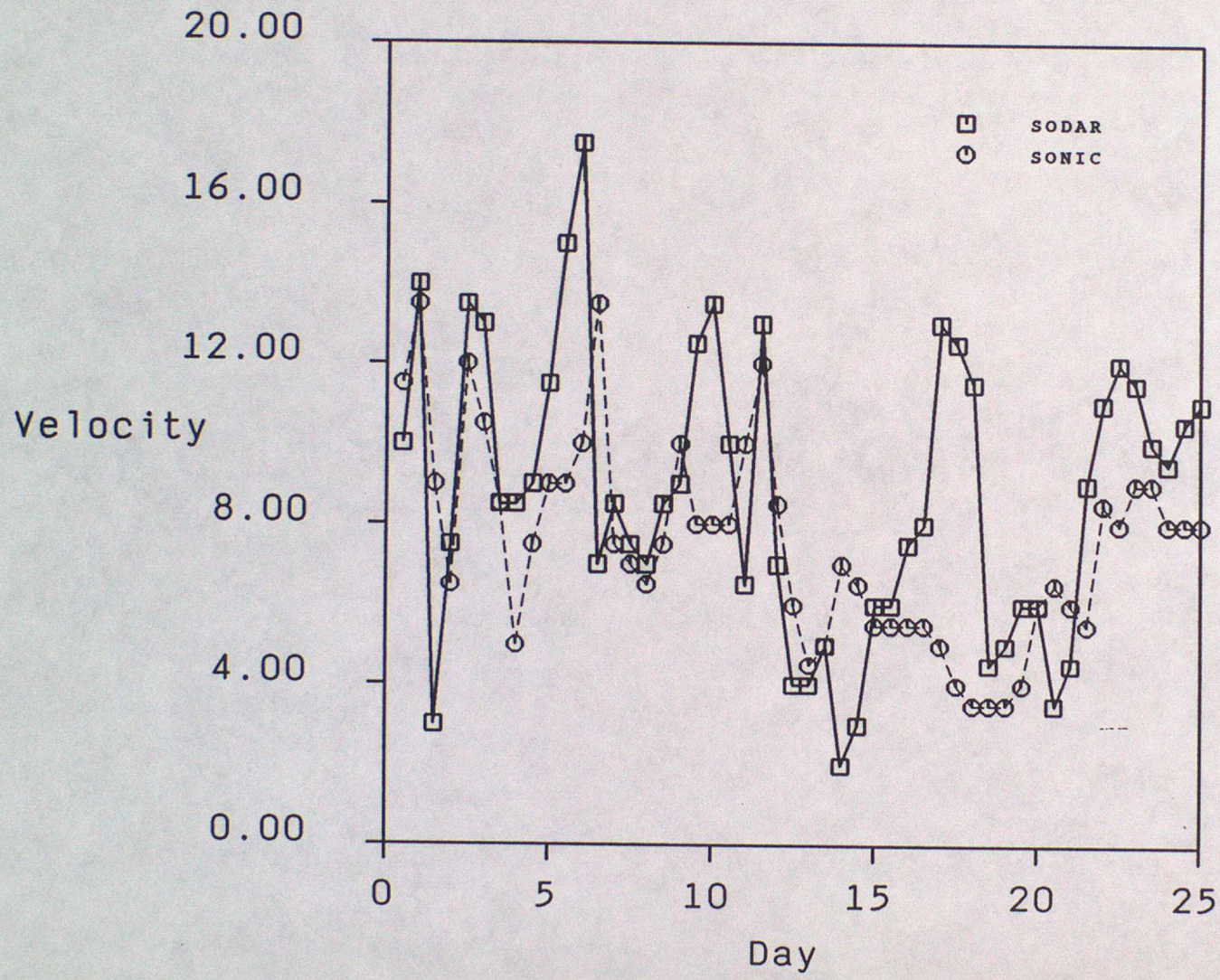

Figure 7: Sodar versus Sonic windspeed for three month periods

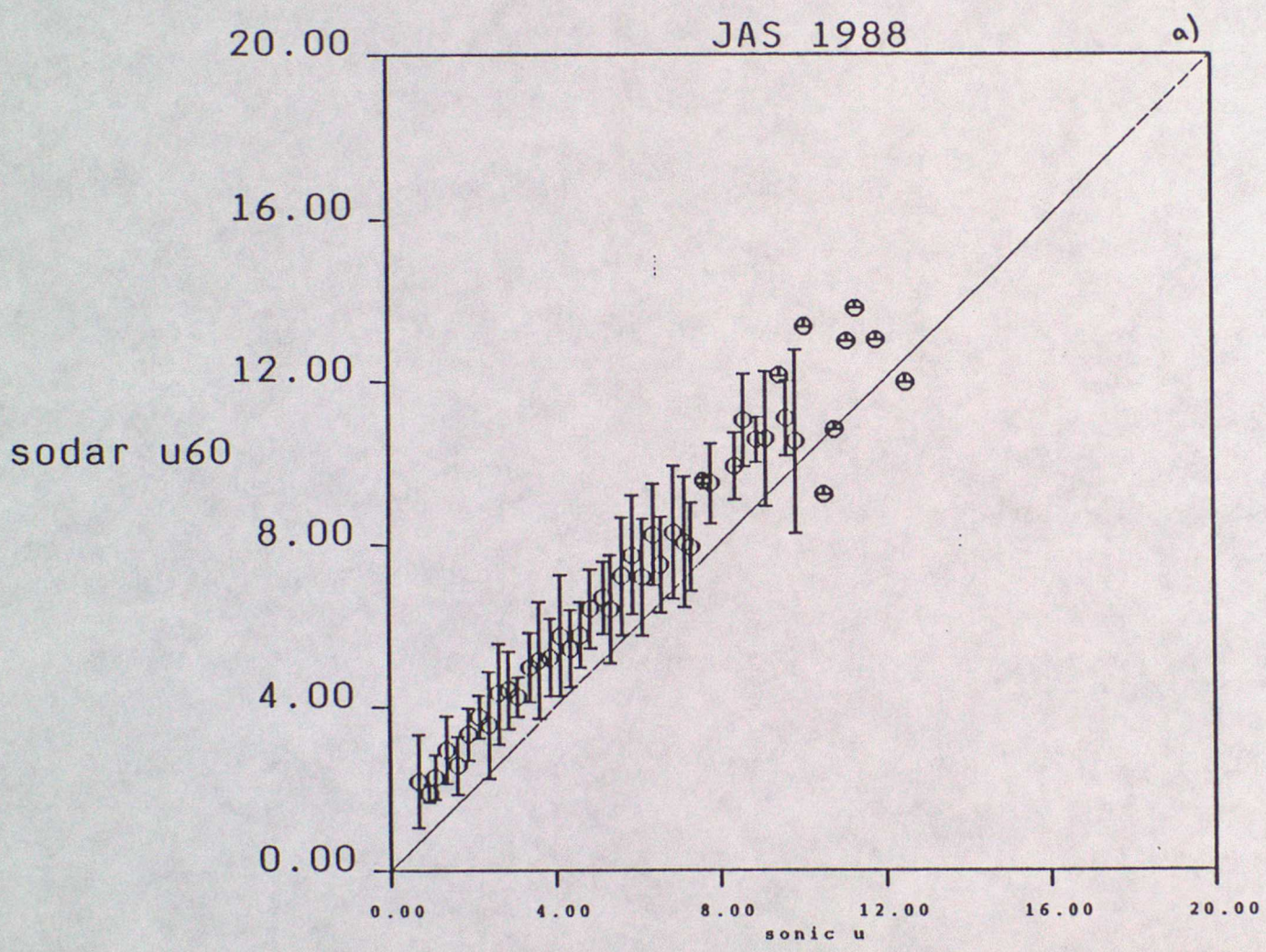

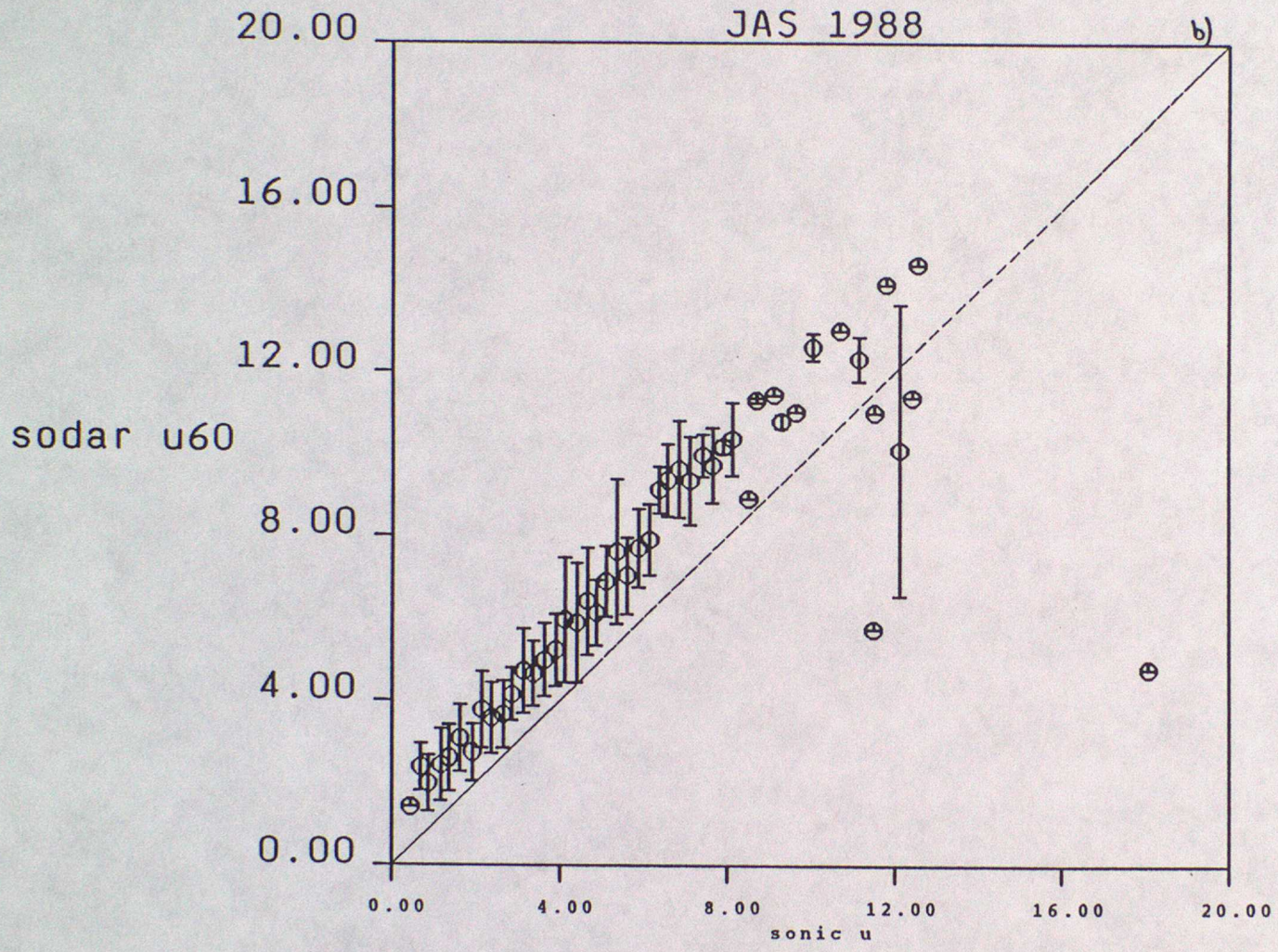
JAS 1988
b)
20.00
16.00
12.00
8.00
4.00
0.00
sodar u60
0.00
4.00
8.00
12.00
16.00
20.00
sonic u

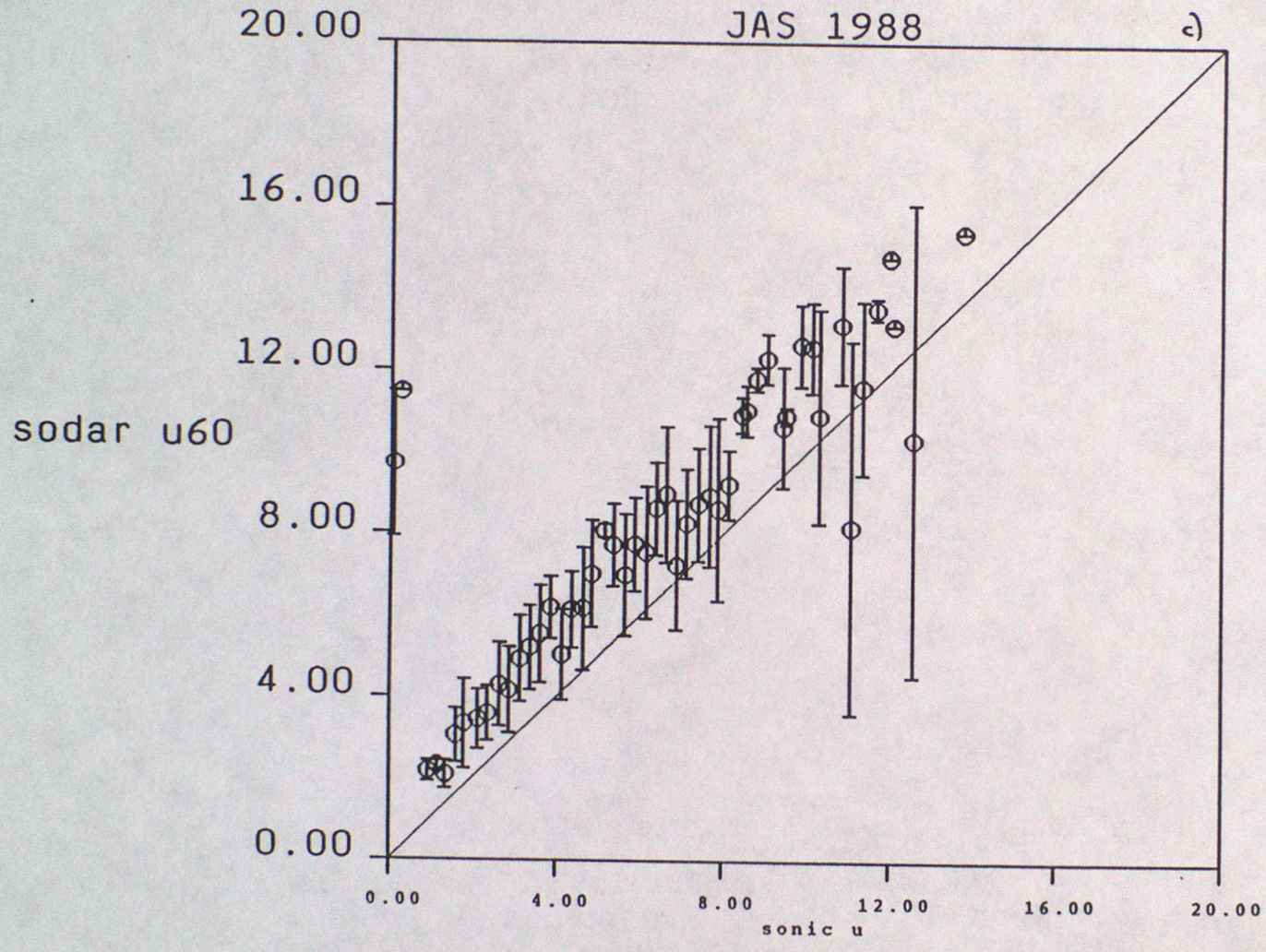
JAS 1988
c)
20.00
16.00
12.00
8.00
4.00
0.00
sodar u60
0.00
4.00
8.00
12.00
16.00
20.00
sonic u

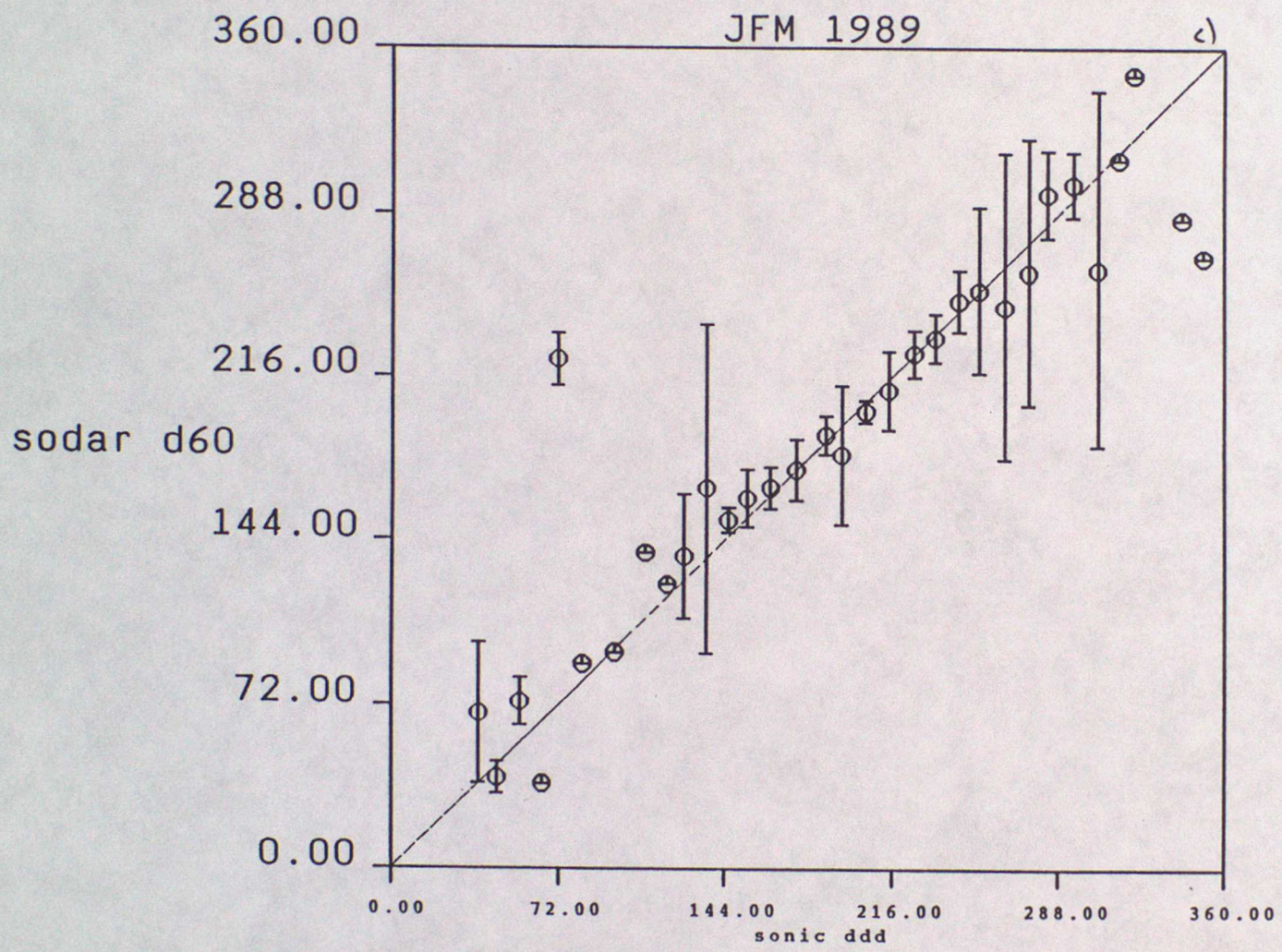
JFM 1989
c)
360.00
288.00
216.00
144.00
72.00
0.00
sodar d60
0.00
72.00
144.00
216.00
288.00
360.00
sonic ddd

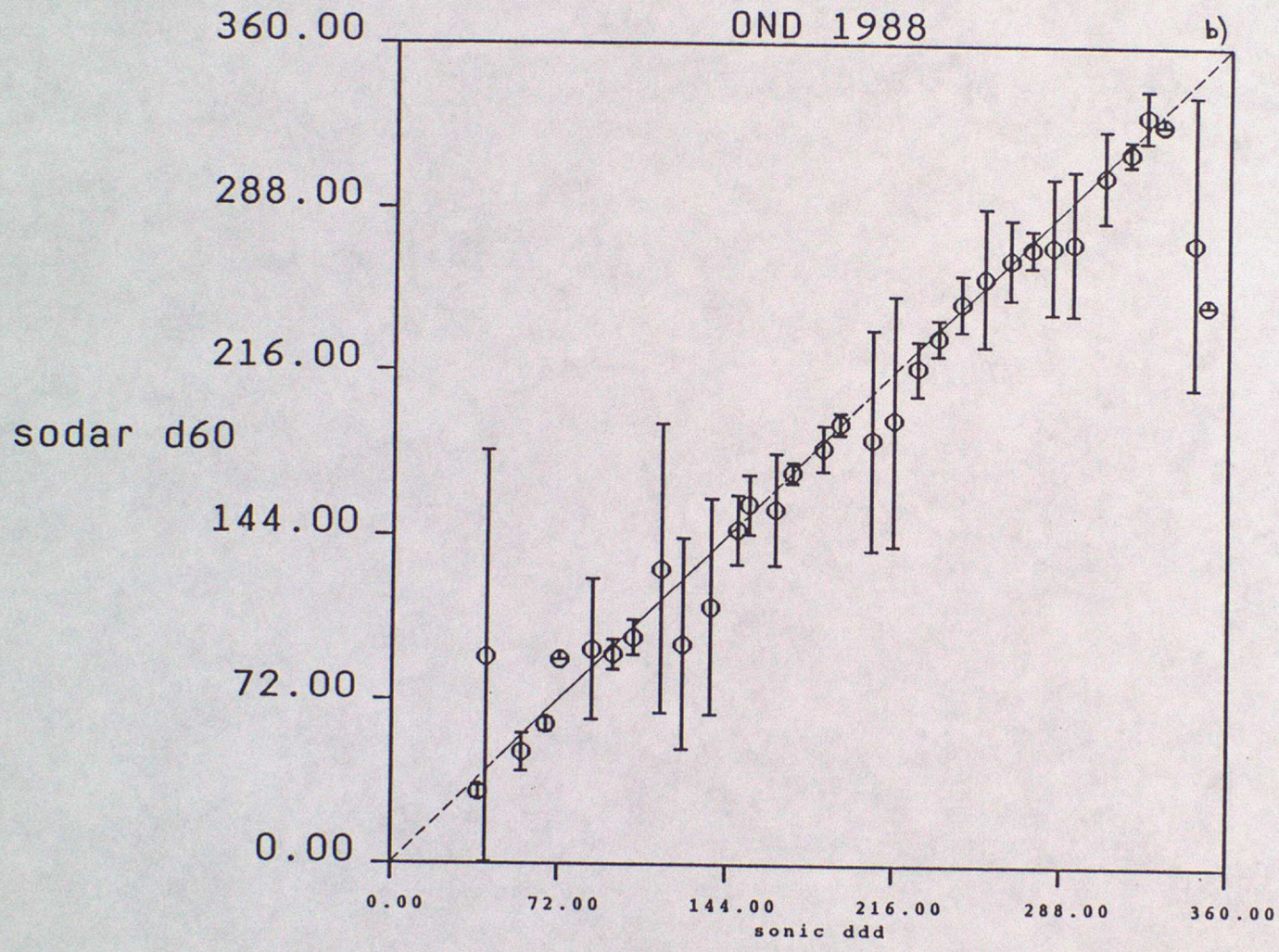
OND 1988
b)
360.00
288.00
216.00
144.00
72.00
0.00
sodar d60
0.00
72.00
144.00
216.00
288.00
360.00
sonic ddd

Figure 8: Sodar versus Sonic direction for three month periods

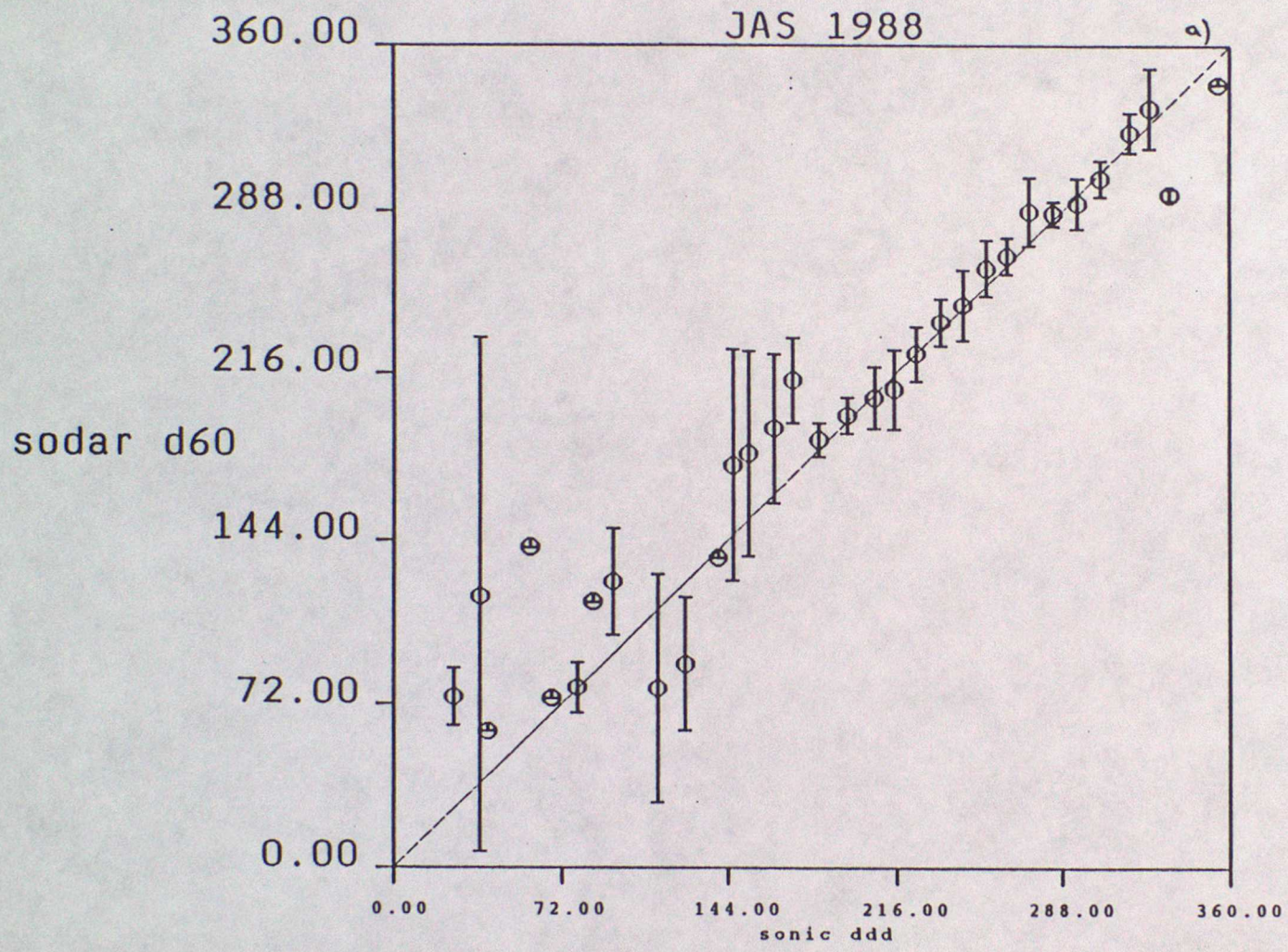

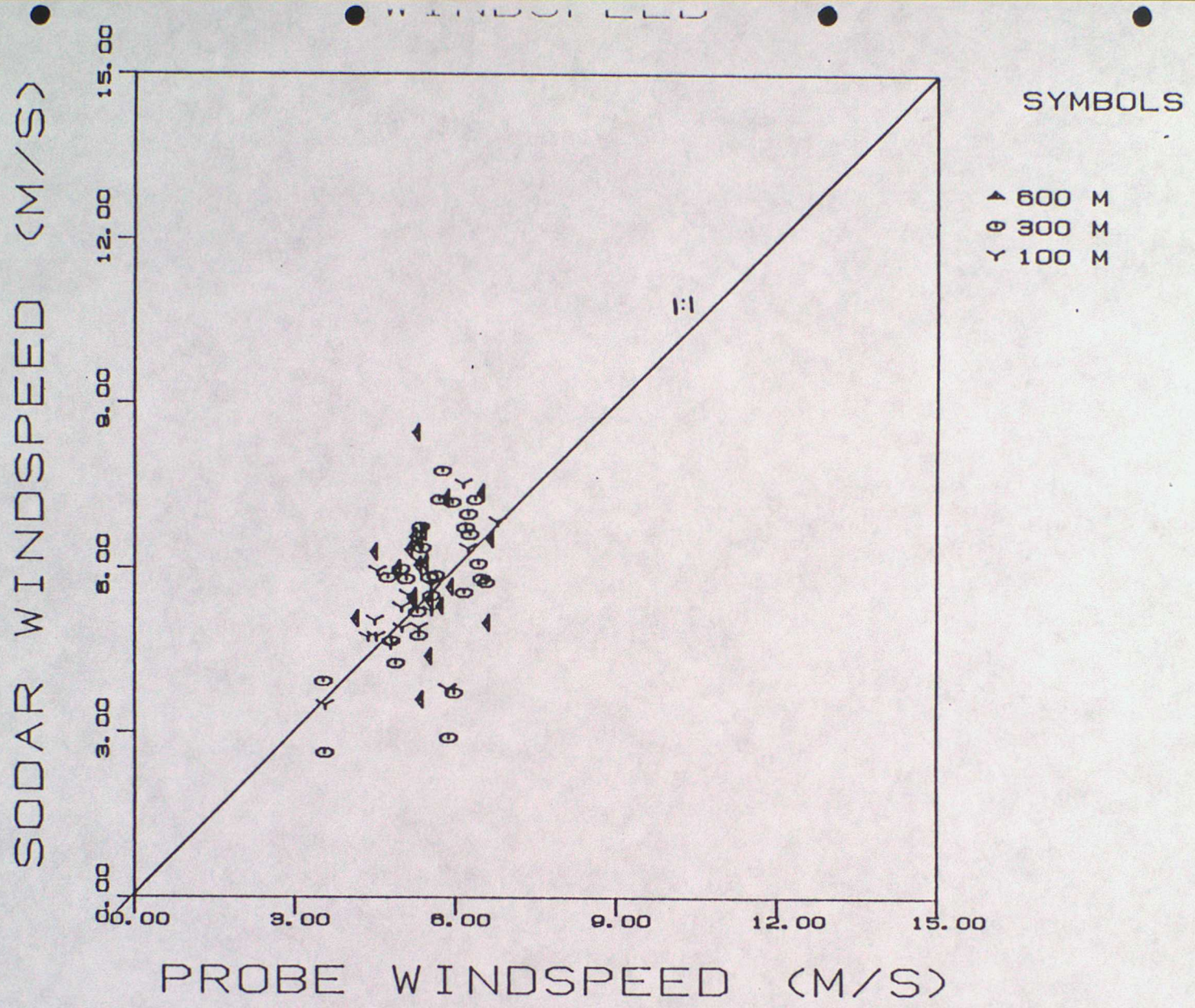

Figure 9: Sodar versus Probe speed

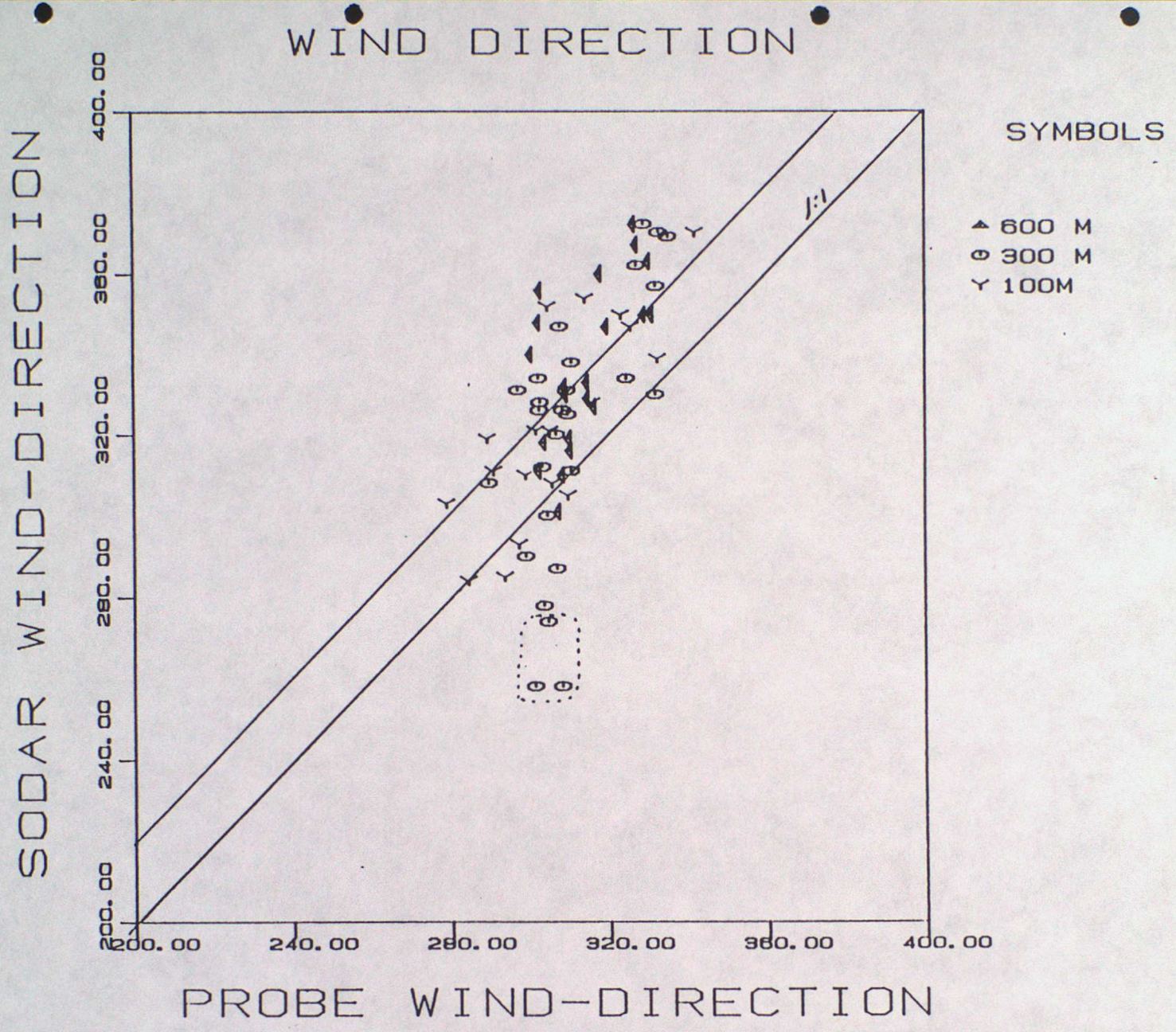

Figure 10: Sodar versus Probe direction

Figure 11: Sodar versus Cabauw Tower speed

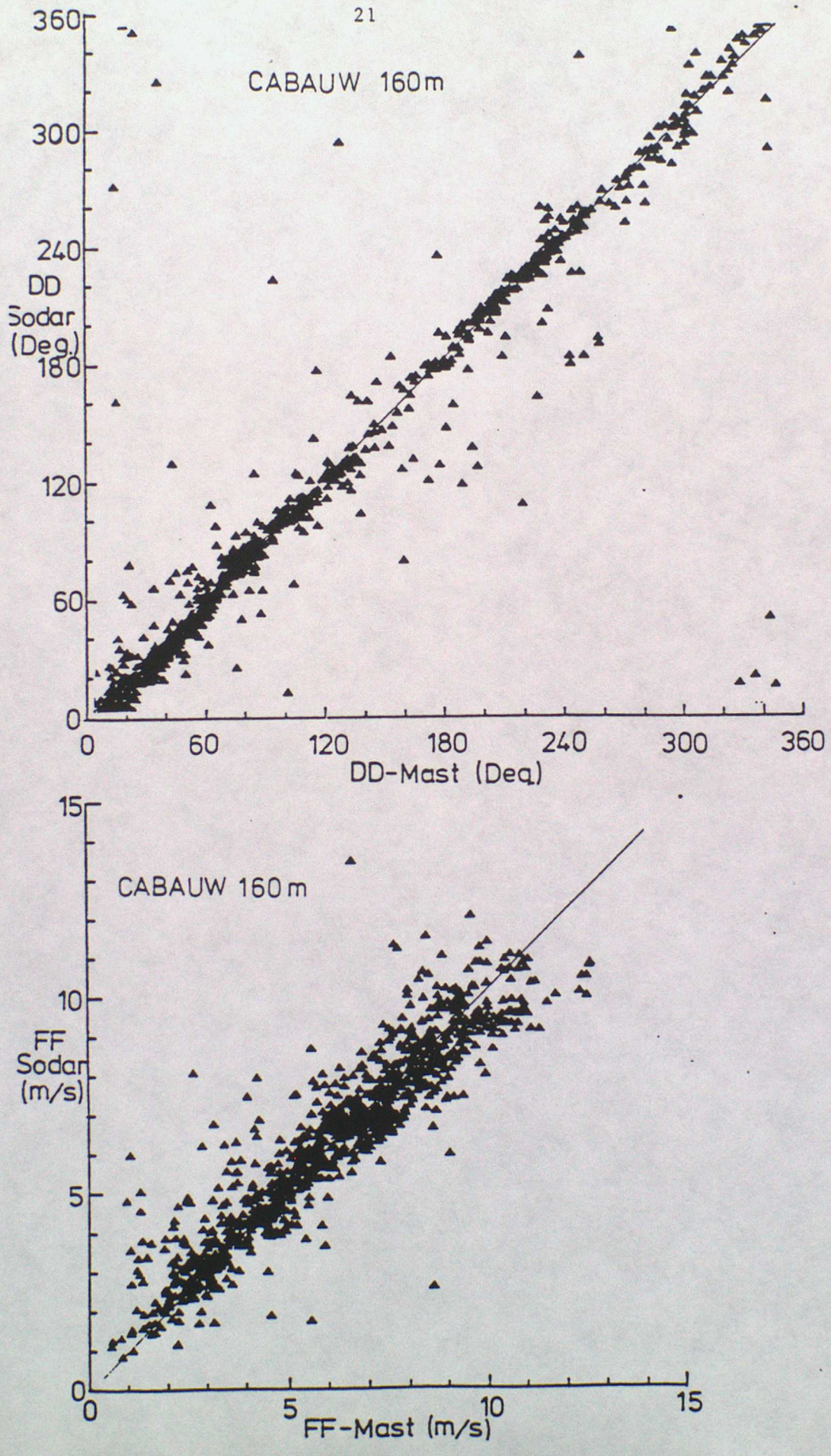

Figure 12: Sodar RMS deviations versus z/L for 60m

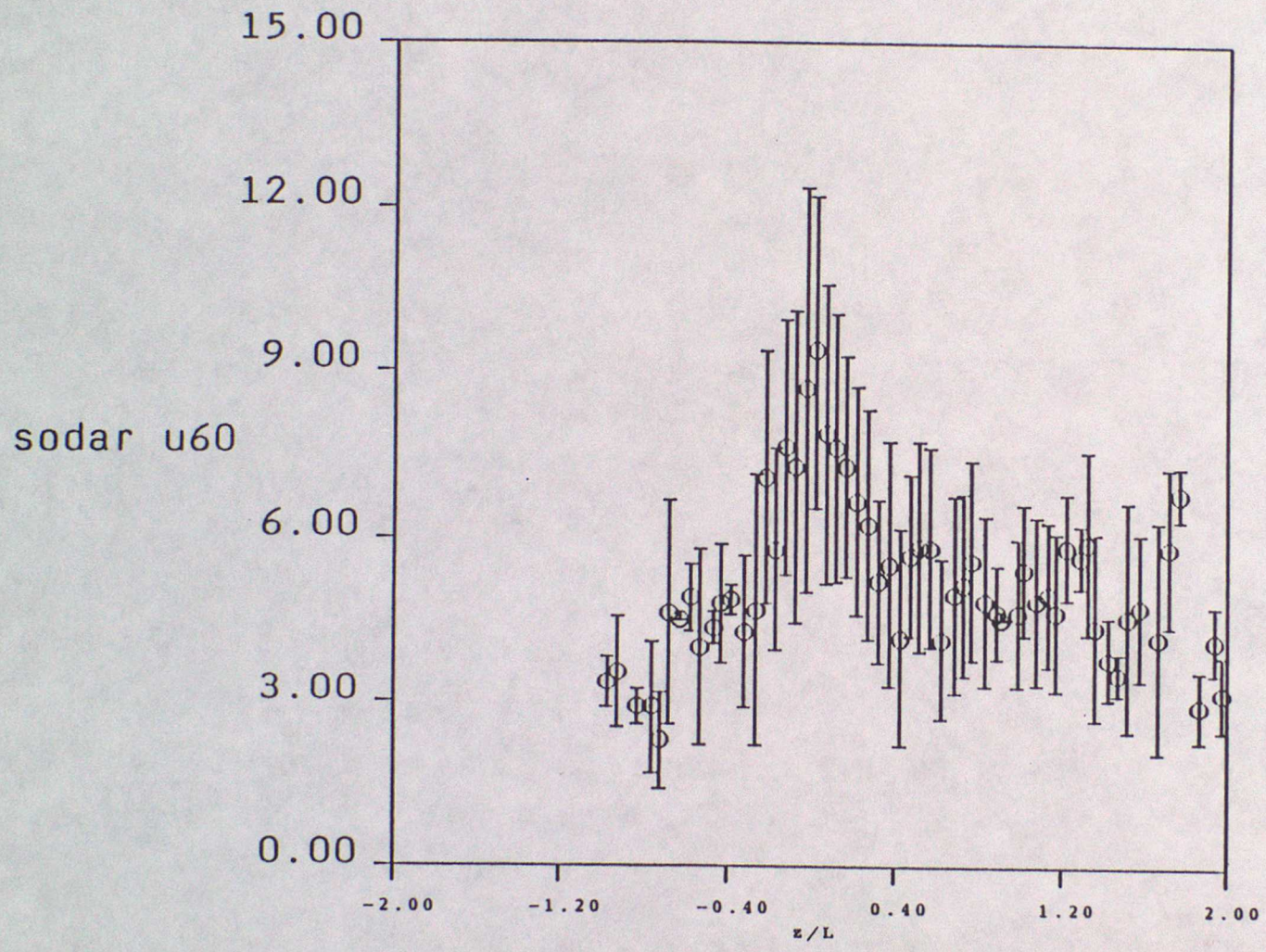

Figure 13: Sodar RMS deviations versus z/L for 100m

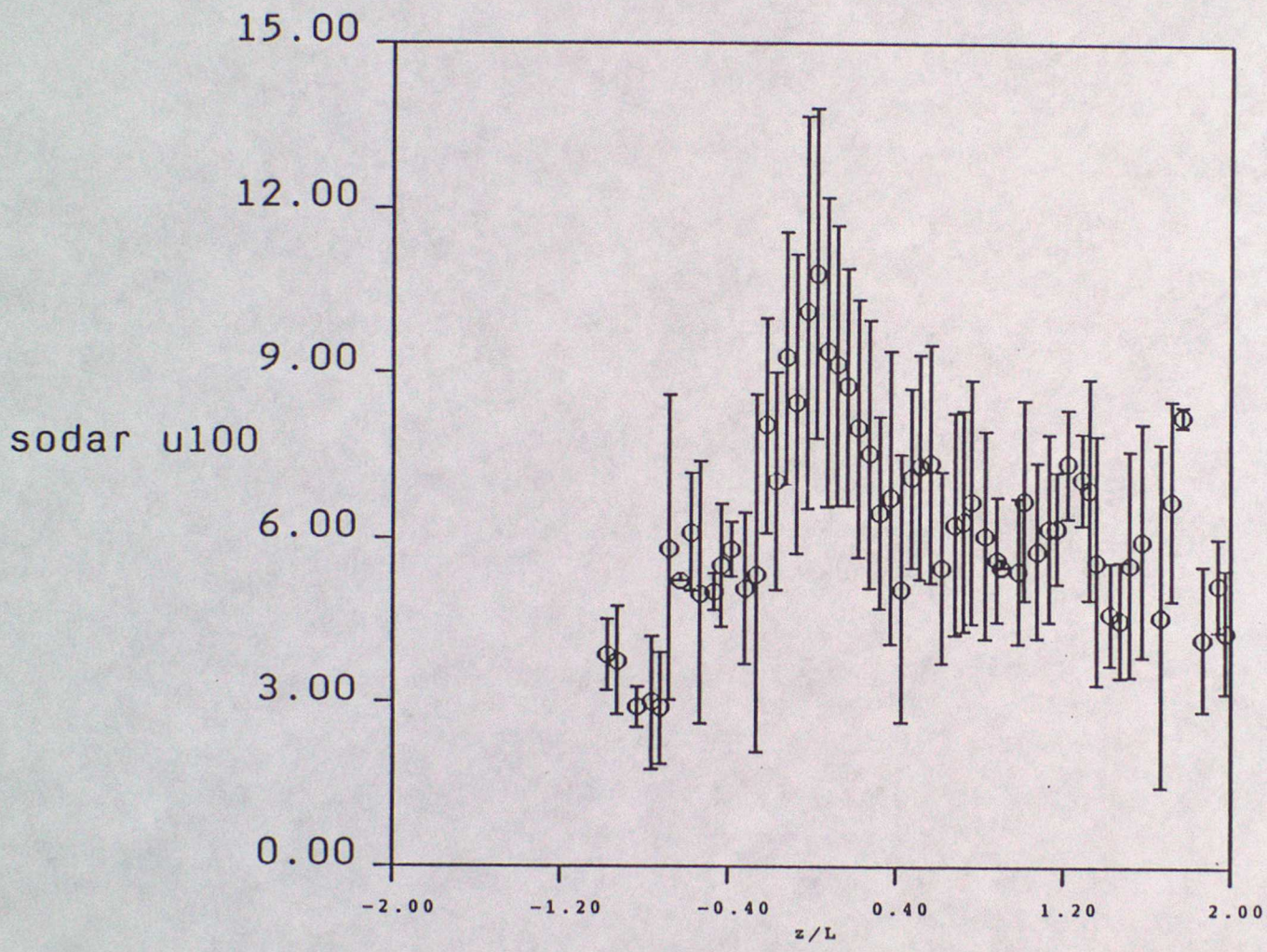

Figure 14: Maximum height versus percentage profiles

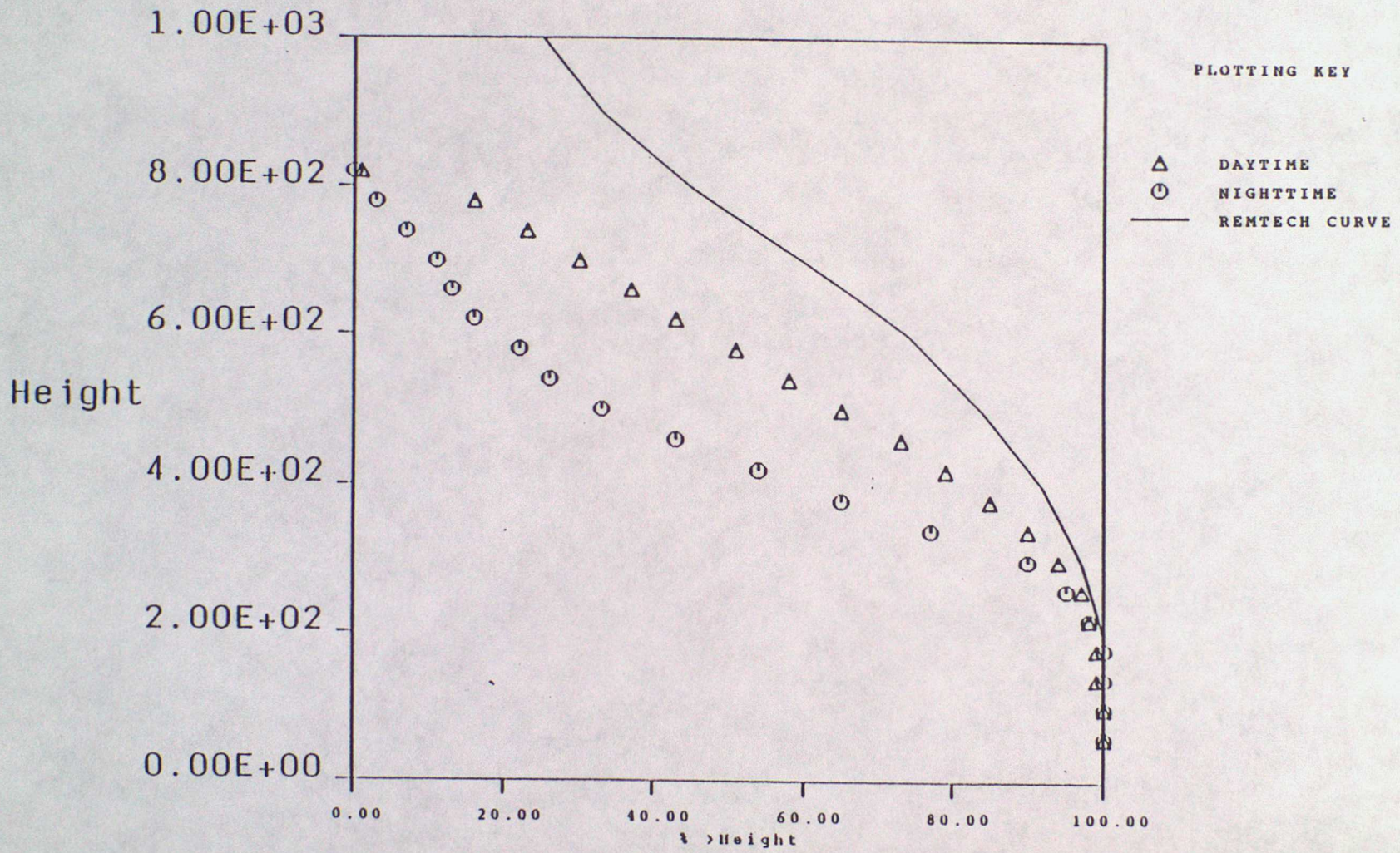

Figure 15: Range versus Windspeed for Period

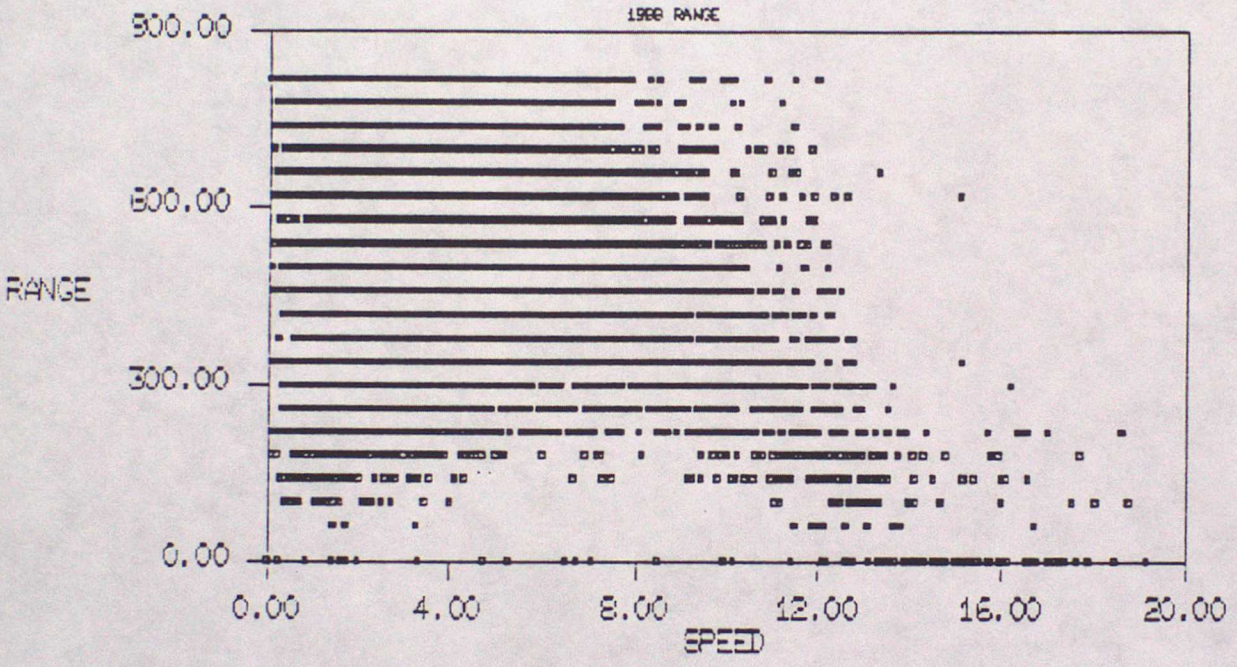

Figure 16: Echo facsimile trace for 10th August 1988

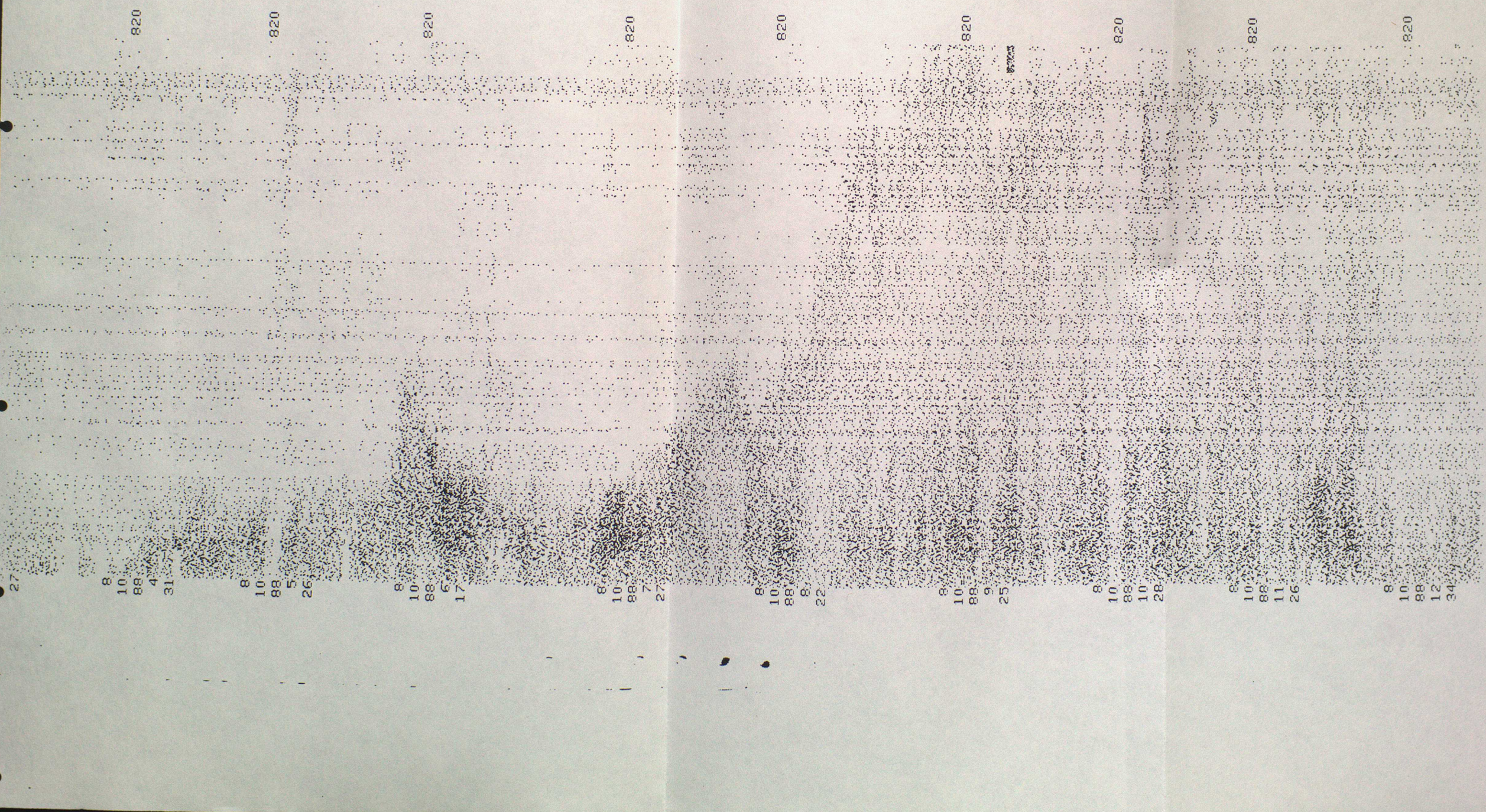

Figure 17: Range for 9th and 10th August 1988

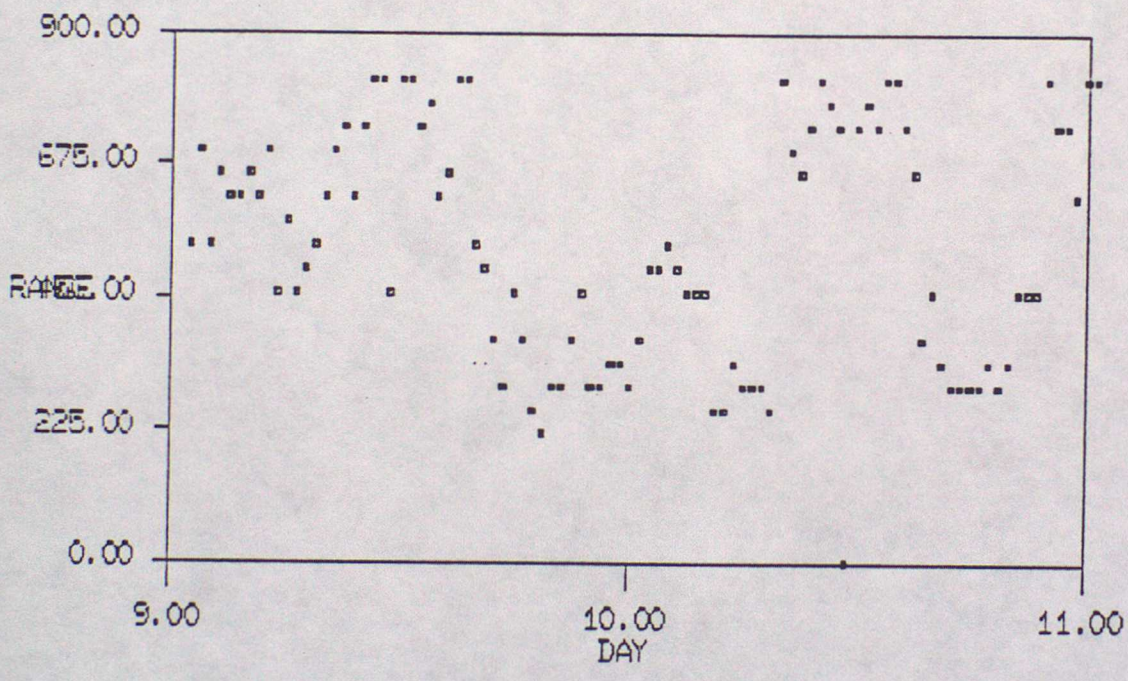

Figure 18: U(h)/U(20) versus height for Neutral conditions